DØ Note 5020-CONF

Search for GMSB SUSY in Diphoton Events with Large Missing E_T with DØ detector

The DØ Collaboration
URL http://www-d0.fnal.gov

(Dated: March 10, 2006)

We report the results of a search for GMSB SUSY in the diphoton final state using 760 pb^{-1} of data collected by the DØ Experiment at the Fermilab Tevatron Collider in 2002-2005. No excess of events above the standard model background has been found, and a lower limit on the lightest neutralino (chargino) mass of 120 (220) GeV has been set at the 95% C.L. These are the most stringent limits in the class of models considered in this analysis to date.

Preliminary Results for Winter 2006 Conferences

1. INTRODUCTION

Low scale supersymmetry (SUSY) is one of the most promising solutions to the hierarchy problem associated with the large disparity between electroweak and Planck scales. It stabilizes the Higgs boson mass and postulates that for each known particle there exists a superpartner. Bosons have fermion superpartners and vice versa. None of the superpartners have been observed so far, so superpartner masses must be much larger than that of their partners, *i.e.* SUSY is a broken symmetry.

Experimental signatures of supersymmetry are determined by the manner and scale of its breaking. In models with gauge-mediated supersymmetry breaking (GMSB) [1, 2] it is achieved by the introduction of new chiral supermultiplets, called messengers, which couple to the ultimate source of supersymmetry breaking, and also to the SUSY particles. At colliders, assuming R-parity conservation [3], superpartners are produced in pairs, and then each decays to the next-to-lightest SUSY particle (NLSP), which can be either a neutralino or a slepton. In the former case, which is considered in this note, the NLSP decays into a photon and a gravitino (the lightest superpartner in GMSB SUSY models, with mass less than $\sim$ 1 keV) which is stable and escapes detection, creating imbalance of the transverse energy in the event. Therefore, the signal we are looking for is a final state with two energetic photons and large missing transverse energy ($\not\!\!E_T$).

The differences in event kinematics between particular GMSB SUSY models result in different experimental sensitivities, so in order to obtain quantitative results we consider a model referred to as Snowmass Slope SPS 8 [4]. This model has only one dimensioned parameter Λ that determines the effective scale of SUSY breaking. The minimal GMSB parameters correspond to a messenger mass $M_m = 2\Lambda$, the number of messengers $N_5 = 1$, the ratio of the vacuum expectation values of the two Higgs fields $\tan\beta = 15$, and the sign of the Higgsino mass term $\mu > 0$. The lifetime of the neutralino is not fixed by this model line, and is assumed to be sufficiently short to result in decays with prompt photons.

GMSB SUSY was searched for at the Tevatron in both Run I [5] and early in Run II [6, 7], as well as by the LEP collaborations [8]. The early Run II limits from DØ and CDF for the SPS 8 were combined [9] to give $\Lambda > 84.6$ TeV, which corresponds to the chargino mass limit of 209 GeV.

This analysis is an update of [6], using about three times more data and with improvements to photon identification, as well as an introduction of an electromagnetic (EM) cluster pointing algorithm, which allows prediction of the vertex position of the photon with a resolution of about 2 cm, effectively eliminating the major instrumental background associated with mis-reconstruction of the primary interaction vertex.

2. DATA ANALYSIS

We use single EM triggers in this analysis. GMSB SUSY events have two energetic photons per event, and we have estimated the trigger efficiency to be $1.00^{+0}_{-0.04}$. We rejected runs with identified instrumental problems with either the calorimeter or the tracker. The total integrated luminosity of the sample is $760 \pm 50\ pb^{-1}$.

2.1. Particle Identification

Photons and electrons are identified in two steps: the selection of the EM clusters, and then separation into photons or electrons. EM clusters are selected from calorimeter clusters by requiring that (i) at least 96% of the energy be deposited in the EM section of the calorimeter, (ii) the calorimeter isolation variable (I) be less than 0.07, where $I = [E_{tot}(0.4) - E_{EM}(0.2)]/E_{EM}(0.2)$, where $E_{tot}(0.4)$ is the total shower energy in a cone of radius $\mathcal{R} = \sqrt{(\Delta\eta)^2 + (\Delta\phi)^2} = 0.4$, and $E_{EM}(0.2)$ is the EM energy in a cone $\mathcal{R} = 0.2$, (iii) the transverse shower profile be consistent with those expected for an EM shower, and (iv) the scalar sum of the p_T of all tracks originating from the primary vertex in an annulus of $0.05 < \mathcal{R} < 0.4$ around the cluster be less than 2 GeV. The cluster is then defined as an electron if there is a reconstructed track pointing to it and a photon otherwise. Jets are reconstructed using the iterative, midpoint cone algorithm [10] with a cone size of 0.5. $\not\!\!E_T$ is determined from the energy deposited in the calorimeter for $|\eta| < 4$ and is corrected for jet and EM energy scales.

2.2. Di-photon Data Sample

We select events with two photons in the central calorimeter ($|\eta_d| < 1.1$) with $E_T > 25$ GeV. We also require that at least one of the photon candidates to have associated preshower hits, and that the primary vertex be consistent with the photon pointing. To ensure robust reconstruction of $\not\!\!E_T$ we also require the direction of $\not\!\!E_T$ not to be back-to-back with the highest jet in the event, $\Delta\phi(jet, \not\!\!E_T) < 2.5$ (if jets are present).

These selections yield 1790 events ($\gamma\gamma$ sample), out of which 1549 events have $\not\!\!E_T < 12$ GeV and four events have $\not\!\!E_T > 45$ GeV. We consider these four events as our SUSY candidates ($\gamma\gamma\not\!\!E_T$ sample). In Figure 1 we display the $\not\!\!E_T$ distribution in the $\gamma\gamma$ sample.

2.3. Backgrounds

Physics backgrounds are estimated to be negligible. Instrumental backgrounds to $\gamma\gamma\not\!\!E_T$ events can be divided into two categories: the ones with and without true $\not\!\!E_T$. The latter are comprised mostly of QCD processes, with either real photons or jets mis-identified as photons. The former ones always involve electron-photon misidentification. The only significant sources of this background are $W(\rightarrow e\nu)\ \gamma$ and $W(\rightarrow e\nu)\ jet$ production, where the electron and the jet are misidentified as a photon.

2.3.1. Backgrounds Without True $\not\!\!E_T$

One can estimate this background using any sample with two EM objects as long as the physics with real missing E_T are suppressed. We use the sample of events that pass exactly the same kinematic and identification cuts as that used to select $\gamma\gamma$ sample, except we loosened the cut on isolation I to 0.12 and require both EM clusters to fail the shower shape cut

The resulting hh sample contains 6114 events; 5172 of them have $\not\!\!E_T < 12$ GeV and 6 events have $\not\!\!E_T > 45$ GeV. Normalizing to the number of events in the $\gamma\gamma\ \not\!\!E_T$ distribution with $\not\!\!E_T < 12$ GeV we calculate the background to

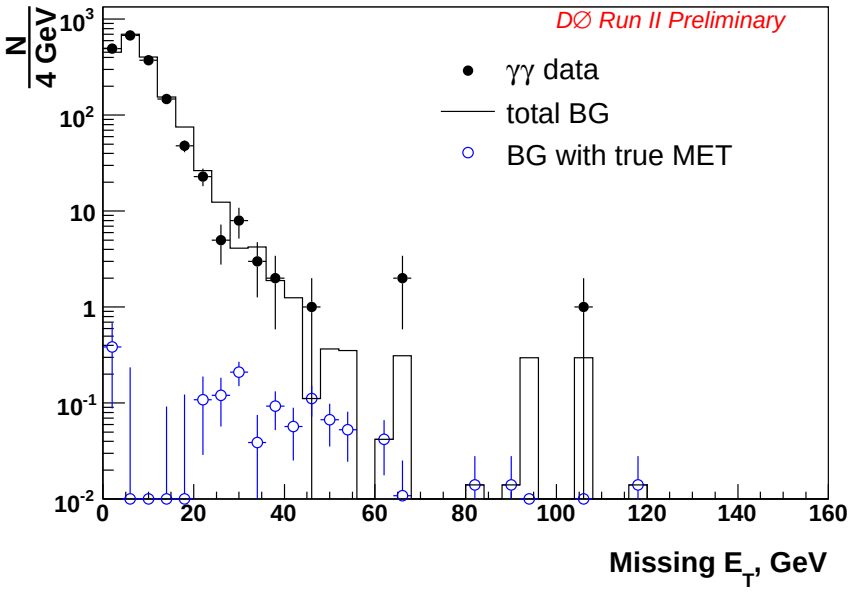

FIG. 1: Missing E_T distribution in the $\gamma\gamma$ sample (black filled points). Black histogram represents the total background, red dashed histogram is background from processes without true $\not\!\!E_T$ and blue open circles show the background from processes with true $\not\!\!E_T$.

the $\gamma\gamma\not\!\!E_T$ sample to be 1.8 ± 0.7 events.

2.3.2. Backgrounds with True $\not\!\!E_T$

This background can be estimated by counting the number of events with electron, photon, and missing E_T and multiplying the result by $(1 - \epsilon_{trk})/\epsilon_{trk}$, where ϵ_{trk} is the track match efficiency. It was measured with $Z \to e^+e^-$ events to be 0.986 ± 0.001. We select the $e\gamma$ sample in exactly the same way as the $\gamma\gamma$ sample, except that the track match requirement on one of the two EM objects is reversed.

The $e\gamma$ sample consists of 1469 events with 1189 having $\not\!\!E_T$ < 12 GeV and 22 with $\not\!\!E_T$ > 45 GeV. First, we remove the contribution of processes without true $\not\!\!E_T$ from the sample. To do this, we use the same procedure as in section 2.3.1 to calculate the background to $e\gamma\not\!\!E_T$ sample (1.4 ± 0.6 events). The total number of events in the $e\gamma\not\!\!E_T$ sample is, therefore 20.6 ± 4.4 events, and the contribution from the backgrounds with true $\not\!\!E_T$ to the $\gamma\gamma\not\!\!E_T$ sample is estimated to be 0.28 ± 0.06 events.

2.3.3. Total Background

Summing up the two background sources, we obtain the total expected background of 2.1 ± 0.7 events (see Table I).

	Total events	$\not\!\!E_T$ < 12 GeV	$\not\!\!E_T$ > 45 GeV
$\gamma\gamma$	1790	1549	4
$e\gamma$	1469	1189	22
hh	6114	5172	6
QCD BG to $\gamma\gamma$			1.8 ± 0.7
QCD BG to $e\gamma$			1.4 ± 0.6
		$e\gamma$ total	20.6 ± 4.4
		$e\gamma$ BG to $\gamma\gamma$	0.28 ± 0.06
Total BG to $\gamma\gamma$			2.1 ± 0.7

TABLE I: The event counts in the $\gamma\gamma$, $e\gamma$, and hh samples, and determination of the total background to diphoton sample.

Λ, TeV	$m_{\chi_1^0}$, GeV	$m_{\chi_1^+}$, GeV	σ_{TOT}^{LO} , fb	K-factor	Efficiency	95% CL Limit, fb
70	93.7	168.2	215.	1.207	0.167 ± 0.025	63.4
75	101.0	182.3	148.	1.197	0.180 ± 0.027	59.2
80	108.5	198.1	97.5	1.187	0.183 ± 0.027	58.0
85	115.8	212.0	65.4	1.177	0.186 ± 0.028	56.9
90	123.0	225.8	41.8	1.167	0.186 ± 0.028	56.9
95	130.2	239.7	29.5	1.157	0.195 ± 0.029	54.2

TABLE II: Points on the GMSB model Snowmass slope: their cross-sections, efficiencies and cross-section limits.

3. SUSY SIGNAL

To estimate the expected yield of signal events we generated MC for the GMSB Snowmass Slope [4] (see Table II). We used ISAJET [11] v 7.58 to determine sparticle masses and branching fractions and PYTHIA v 6.202 [12] with CTEQ6L1 [13] structure functions for event generation. The interface is described in [14]. The events were then processed through a full detector simulation, reconstructed and processed with the same analysis program as the data.

The dominant contributions to the cross section for all of the points are second neutralino-first chargino and first chargino pair production. The total cross section in Table II is the leading order PYTHIA [12] cross section. The K-factor is applied to get a next-to-leading-order (NLO) cross section. The values of the K-factor in the table are taken from [15].

The uncertainty of the signal efficiency comes from uncertainties of the EM identification (10%), MC statistics (5%), trigger efficiency (4%), track match veto (3%) and PDF (4%).

Figure 2 shows MET distribution for three points on the Snowmass Slope.

4. LIMIT

As the observed numbers of events for all values of $\not\!\!E_T$ are in good agreement with the standard model, we set an upper limit on GMSB SUSY production.

Limits are set by using the standard prescription [16] (uses a Bayesian approach) and are shown in Table II and in

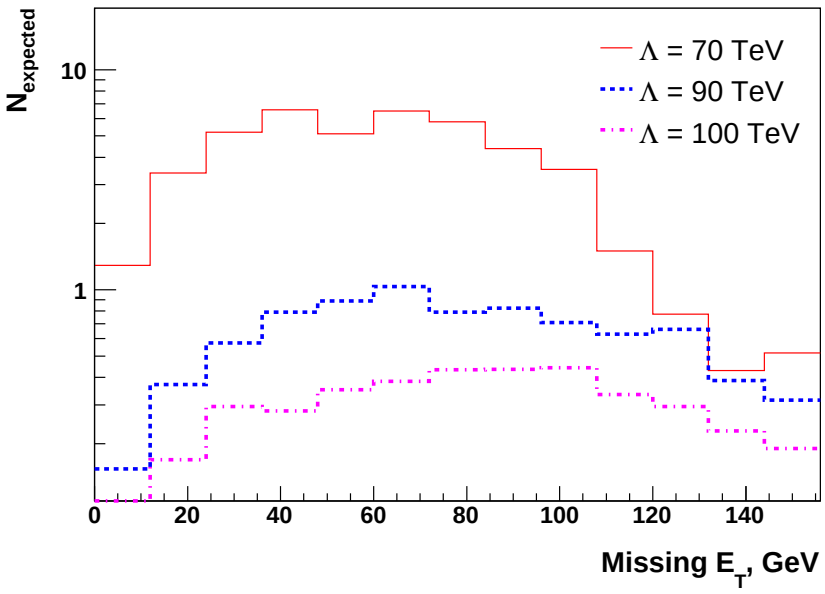

FIG. 2: Expected missing E_T distribution in GMSB SUSY events passing all analysis cuts except $\not\!\!E_T$ for $\Lambda = 70,\ 90, 100\ TeV$.

Fig. 3. The limit is $\Lambda > 88.5$ TeV at 95% confidence level (C.L.), or in terms of gaugino masses, $m_{\chi_1^0} > 120$ GeV and $m_{\chi_1^+} > 220$ GeV.

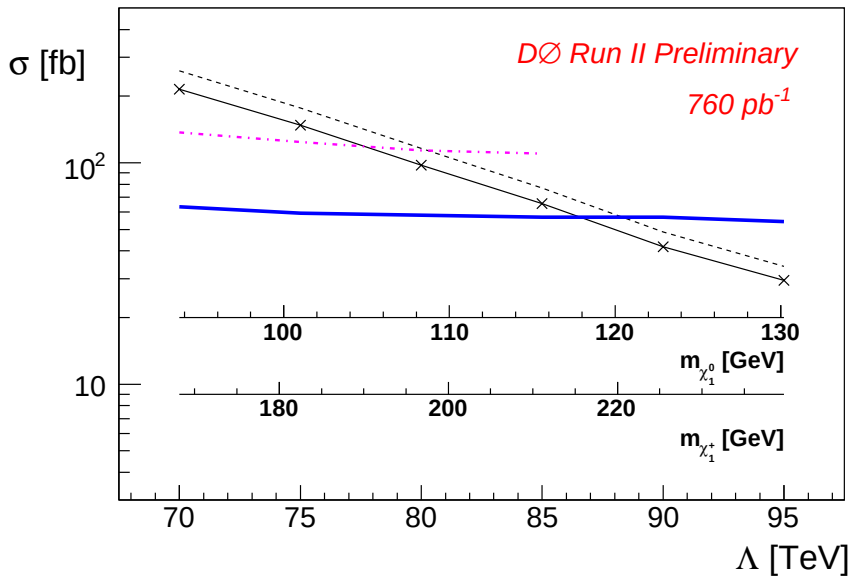

FIG. 3: 95% C.L. limit on GMSB SUSY Snowmass Slope obtained in this analysis (thick blue line) and in the previous DØ result (dot-dashed purple line). SUSY LO (NLO) cross-section is shown in black solid (dashed) line.

[1] P. Fayet, Phys. Lett. B **70**, 461 (1977); *ibid.* **86**, 272 (1979); *ibid.* **175**, 471 (1986).

[2] M. Dine, A. E. Nelson, Y. Nir and Y. Shirman, Phys. Rev. D **53**, 2658 (1996); H. Baer, M. Brhlik, C. H. Chen and X. Tata, Phys. Rev. D **55**, 4463 (1997); H. Baer, P. G. Mercadante, X. Tata and Y. L. Wang, Phys. Rev. D **60**, 055001 (1999); S. Dimopoulos, S. Thomas and J. D. Wells, Nucl. Phys. B **488**, 39 (1997); J. R. Ellis, J. L. Lopez and D. V. Nanopoulos, Phys. Lett. B **394**, 354 (1997);
see also a review by G. F. Giudice and R. Rattazzi, "Gauge-Mediated Supersymmetry Breaking" in G. L. Kane: *Perspectives on Supersymmetry*, World Scientific, Singapore (1998), p. 355-377, and references therein.

[3] G.R. Farrar and P. Fayet, Phys. Lett. **B79** (1978) 442.

[4] S. P. Martin, http://zippy.physics.niu.edu/modellineE.html;
S. P. Martin, S. Moretti, J. M. Qian and G. W. Wilson, "Direct Investigations of Supersymmetry: Subgroup summary report," in *Proceedings of the APS/DPF/DPB Summer Study on the Future of Particle Physics (Snowmass 2001),* edited by N. Graf, eConf **C010630**, p. 346 (2001);
B. C. Allanach *et al.*, Eur. Phys. J. C **25**, 113 (2002).

[5] B. Abbott *et al.* (DØ Collaboration), Phys. Rev. Lett. **80**, 442 (1998).
F. Abe *et al.* (CDF Collaboration), Phys. Rev. D **59**, 092002 (1999).

[6] V. Abazov *et. al.* PRL **94**, 041801 (2005); Y. Gershtein, S. Kesisoglou D0Notes 4344, 4378.

[7] D. Acosta *et. al.* PRD **71** 031104(R) (2005).

[8] LEPSUSYWG, ALEPH, DELPHI, L3 and OPAL Collaborations, note LEPSUSYWG/04-09.1 (http://lepsusy.web.cern.ch/).

[9] V. Buescher *et al.* (CDF and DØ Collaborations), hep-ex/0504004

[10] G. C. Blazey *et al.*, in *Proceedings of the Workshop: "QCD and Weak Boson Physics in Run II"* edited by U. Baur, R. K. Ellis, and D. Zeppenfeld, 47 (2000). See Section 3.5 for details.

[11] F. E. Paige, S. D. Protopescu, H. Baer and X. Tata, hep-ph/0312045.

[12] T. Sjöstrand *et al.*, Computer Physics Commun. **135** (2001) 238.

[13] H. L. Lai *et al.*, (CTEQ Collaboration), Eur. Phys. J. **C** 12 (2000) 375-392.

[14] http://www-d0.fnal.gov/computing/MonteCarlo/generator_tools/susy_tools.html

[15] W. Beenakker *et al.*, Phys. Rev. Lett. **83**, 3780 (1999).

[16] I. Bertram *et al.* FERMILAB-TM-2104.